

which are two time constants

$$1/T_{1a} = W + \frac{1}{2}R + (W^2 + \frac{1}{4}R^2)^{1/2},$$

$$1/T_{1b} = W + \frac{1}{2}R - (W^2 + \frac{1}{4}R^2)^{1/2}.$$

The eigenvalue $1/T_{1a}$ has as an eigenvector

$$\begin{pmatrix} \cos \frac{1}{2}\alpha \\ -\sin \frac{1}{2}\alpha \end{pmatrix},$$

and $1/T_{1b}$, the eigenvector

$$\begin{pmatrix} \cos \frac{1}{2}\alpha \\ \sin \frac{1}{2}\alpha \end{pmatrix},$$

where $\tan \alpha = 2W/R$.

Thus the most general solution to the homogeneous equation is written as

$$\begin{pmatrix} n(t) \\ p(t) \end{pmatrix} = A e^{-t/T_{1a}} \begin{pmatrix} \cos \frac{1}{2}\alpha \\ -\sin \frac{1}{2}\alpha \end{pmatrix} + B e^{-t/T_{1b}} \begin{pmatrix} \cos \frac{1}{2}\alpha \\ \sin \frac{1}{2}\alpha \end{pmatrix},$$

where A and B are arbitrary constants.

The solution to the inhomogeneous part is obtained

in the standard way to obtain the complete solution, where A and B become

$$A = (e^{t/T_{1a}} - 1) T_{1a} p^0 R / 2 \sin \frac{1}{2}\alpha + A_0,$$

$$B = (e^{t/T_{1b}} - 1) T_{1b} p^0 R / 2 \sin \frac{1}{2}\alpha + B_0,$$

where A_0 and B_0 are determined by the initial conditions and given by

$$A_0 = \frac{1}{2} [n(0)/\cos \frac{1}{2}\alpha - p(0)/\sin \frac{1}{2}\alpha],$$

$$B_0 = \frac{1}{2} [n(0)/\cos \frac{1}{2}\alpha + p(0)/\sin \frac{1}{2}\alpha],$$

where $n(0)$ and $p(0)$ are the excitation number for the spin system and phonon system, respectively, at time zero.

Therefore the first component of this vector solution gives us for the time dependence of the spin-system excitation number

$$n(t) = \frac{1}{2} \{ n(0) - \cot \frac{1}{2}\alpha [p(0) - p^0 T_{1a} R] \} e^{-t/T_{1a}} + \frac{1}{2} \{ n(0) + \cot \frac{1}{2}\alpha [p(0) - p^0 T_{1b} R] \} e^{-t/T_{1b}}.$$

†Research sponsored by the U. S. Air Force under Grant No. AF-AFOSR-450-66 and the Advanced Research Projects Agency under Contract No. SD-100.

*Present address: American Enka Company, Enka, N. C. 28728.

¹*Spin-Lattice Relaxation in Ionic Solids*, edited by A. A. Manenkov and R. Orbach (Harper and Row, New York, 1966).

²A. Abragam, *The Principles of Nuclear Magnetism* (Oxford U. P., London, 1961).

³See Ref. 1, pp. 260-289.

⁴E. L. Hahn, *Phys. Rev.* **80**, 450 (1950).

⁵P. L. Scott and C. D. Jeffries, *Phys. Rev.* **127**, 32 (1962).

⁶A. A. Manenkov, V. A. Milyaev, and A. M. Prokhorov, *Fiz. Tverd. Tela* **4**, 388 (1962) [*Sov. Phys. Solid State* **4**, 280 (1962)]; R. L. Sanders and L. G. Rowan, *Phys. Rev. Letters* **21**, 140 (1968).

⁷R. H. Dicke, *Phys. Rev.* **93**, 99 (1954).

⁸E. R. Buley and F. W. Cummings, *Phys. Rev.* **134**, A1454 (1964).

⁹S. L. McCall and E. L. Hahn, *Phys. Rev.* **183**, 457 (1969); N. S. Shiren, *Phys. Rev. B* **2**, 2471 (1970).

Multiple Scattering of Heavy Ions of keV Energies Transmitted through Thin Carbon Films

H. H. Andersen and J. Böttiger

Institute of Physics, University of Aarhus, DK 8000 Aarhus C, Denmark

(Received 6 May 1971)

This paper describes experimental studies of multiple scattering of 13 different heavy ions with $3 \leq Z_1 \leq 30$ in the energy range of 200-1000 keV, transmitted through thin ($8-25 \mu\text{g}/\text{cm}^2$) carbon foils. The agreement between our experimental data, recent theoretical calculations, and published experimental data is found to be satisfactory, although a small systematic deviation exists for thicker foils.

I. INTRODUCTION

For several years, multiple scattering of light ions of high energies has been extensively studied.¹ Recently, there has been a growing interest in the investigation of multiple scattering in very thin foils at energies low enough for a classical theoret-

ical treatment to be applicable.² This interest is motivated both experimentally and theoretically.

A knowledge of multiple-scattering angular distributions is necessary in several cases. For example, in experiments with heavy ions, multiple scattering very often appears as an undesirable process decreasing the resolution of the experi-

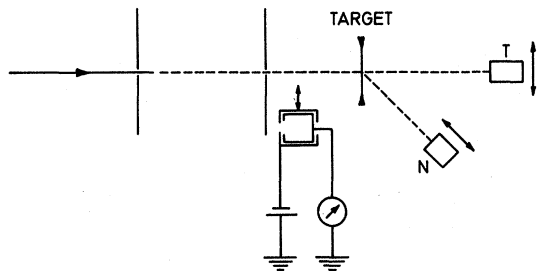


FIG. 1. Schematic diagram of experimental setup. N and T are solid-state surface-barrier counters. The beam divergence is better than 0.1° . The acceptance solid angle of counter T is 2×10^{-6} .

ment (e.g., beam-foil spectroscopy³ and channeling⁴). Also in the construction of heavy-ion accelerators, the multiple scattering in possible stripper foils must be known in order to calculate the transmission efficiency for the accelerator.

The study of multiple scattering of heavy ions of keV energies is also of basic theoretical interest. Primarily, it yields information on the scattering of projectiles on target atoms for scattering angles where a screened Coulomb potential must be used to describe the interaction. Furthermore, Bohr⁵ showed that there is a close connection between the half-width of the multiple-scattering distribution and the energy loss in nuclear collisions. Thus multiple-scattering data can be used to yield information on nuclear stopping power—a parameter which for most ion-target combinations is considerably more difficult to measure.

The basic theoretical paper on the subject of multiple scattering is that of Molière.⁶ In the region of thin foils and low projectile energies, his results are not well suited for a direct comparison with experiment. Meyer⁷ simplified the treatment by assuming classical scattering from the beginning of the calculations. He expressed his results as a unique function, connecting a reduced half-width with a reduced thickness. Extensive experimental data are necessary for testing the scaling of angle and thickness involved in this theory.

The present paper describes experimental studies of multiple scattering of 13 different heavy ions with $3 \leq Z_1 \leq 30$ in the energy range 200–1000 keV transmitted through 8–25- $\mu\text{g}/\text{cm}^2$ carbon foils. The choice of many different incident ions allowed an extensive test of the scalings inherent in Meyer's theory. The agreement between our experimental data, the results of Meyer's calculations, and other experimental data is found to be very satisfactory.

II. EXPERIMENTAL

A. Experimental Setup

The purpose of the experimental study was (i) to

measure the angular distribution of heavy ions transmitted through thin carbon films, and (ii) to measure the corresponding foil thickness. The same experimental equipment was used for both experiments.

A schematic representation of the apparatus is shown in Fig. 1. Two collimators define the direction and divergence ($\leq 0.1^\circ$) of the beam from the Aarhus 600-kV heavy-ion accelerator. The beam currents incident on the targets were measured with a movable Faraday cup, designed with suitable secondary electron suppression. The currents ($\sim 10^{-11}$ A) used when measuring multiple-scattering distributions were lower than the limit for obtaining accurate current readings, and currents were thus measured only in connection with thickness determinations. The targets were self-supporting thin carbon films mounted on aluminum frames. The diameter of the self-supporting part of the thin film was 3 mm, and that of the beam spot 1 mm. No separate pumping facility was connected to the scattering chamber, and the pressure around the target was $5\text{--}15 \times 10^{-6}$ Torr.

The movable detector T , which has a small solid angle ($\sim 2 \times 10^{-6}$) as seen from the target, was used to scan through the transmitted beam to derive the multiple-scattering distributions. An accurate gearing system gives T two perpendicular motions. The shafts were provided with potentiometers from which analog signals, indicating the positions to approximately 0.2 mm, may be obtained. This corresponds to an angular resolution of 0.05° . A detector N measured the yield of particles scattered to $\sim 45^\circ$ and was used for normalization. In order to obtain a reasonable ratio between the counting rates in N and T , the distance of N from the target was adjustable. Both detectors (N and T) were standard Ortec surface-barrier solid-state counters. Standard electronics were used for detection and energy analysis.

B. Discussion of Measuring Procedure

1. Angular Distributions

To obtain the ratio (C_T/C_N) between the counting rates in T and N as a function of the position T , the following method was adopted: The indication of the scaler connected to T was fed through a digital-to-analog converter to the y axis of an x - y recorder. The analog signal from one of the position potentiometers was connected to the x axis of the same recorder on which the angular distribution was thus directly recorded. For normal running conditions, the determination of the half-widths of the angular distributions are accurate within a few percent. The uncertainty is mainly due to counting statistics.

On some occasions when isotopes neighboring the one used were very abundant, a rather large

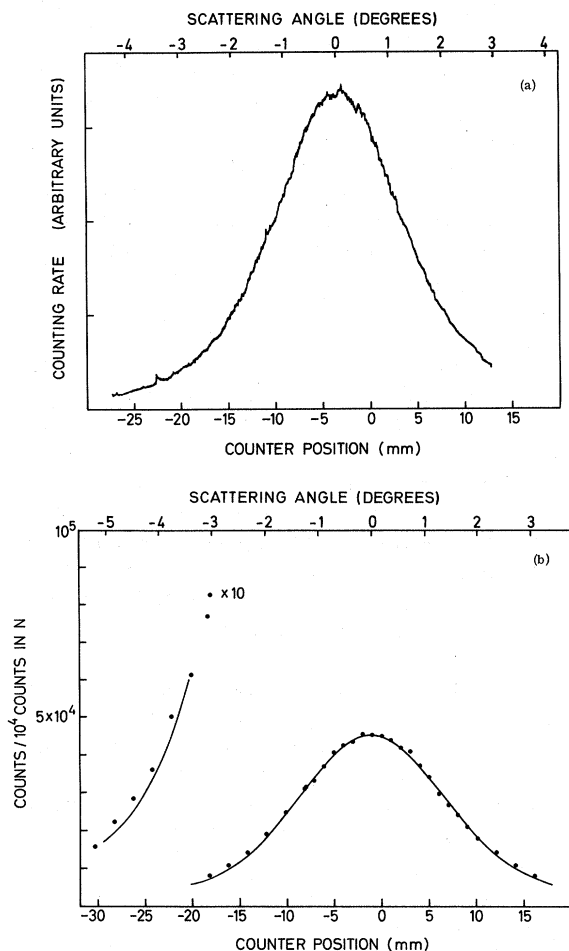


FIG. 2. (a) A typical angular distribution for 500-keV ^{20}Ne transmitted through a thin carbon foil ($13.1 \mu\text{g}/\text{cm}^2$). The ratemeter belonging to counter T is connected directly to the recorder. The distance from the target to the counter T (at zero scattering angle) is 323 mm. (b) A typical angular distribution for 500-keV ^{32}S transmitted through a thin carbon foil ($8.66 \mu\text{g}/\text{cm}^2$). The digital-to-analog converter is connected to the recorder. The full line is the corresponding theoretical distribution as given by Eq. (5).

amount of ions from these isotopes may reach N via scattering from chamber walls, etc. As this detector spans a rather large interval of scattering angles, the resolution of the peak belonging to the primary beam was usually poor and, in contrast to what was the case for T , it was often impossible to get rid of the influence from the contamination through energy discrimination. As long as the ratio between the contamination and the primary beam does not change, this will not influence the results. In order to test this, some data points from various parts of the distribution were repeated after each run. If agreement within the counting statistics was not obtained, the entire distribution was

discarded. It took 10–30 min to measure a distribution, and it was not always possible to obtain reproducible results. In such cases, provided the intensity of the primary beam could be stable for 5 min, we connected the T ratemeter directly to the y axis of the recorder without using detector N . Typical measured angular distributions obtained by either method are shown in Fig. 2.

Besides the isotope under investigation, the incident beam in a few cases also contained molecular compounds or doubly-charged ions with a mass which was half that of the wanted isotope, but with an energy twice as large, etc. It was normally possible to eliminate the contribution to the angular distributions from the "impurity" isotopes by placing energy windows in the analyzer of detector T . Even with the heavy ions used, energy information could still be obtained from the pulses of the solid-state detector when 500-keV incident energy was used, but a large energy loss in the detector dead-layer and a decreased resolution were observed.

2. Thickness Measurements

The thicknesses were obtained by comparing large-angle scattering yields in detector T (for He ions scattered in the target) with the incident current as measured with the Faraday cup. Assuming that the He ions were Rutherford scattered in the target, the thicknesses can be derived by means of Rutherford-scattering cross section.

To carry out such a measurement, the geometry (scattering angle and solid angle of the detector as seen from the target) has to be carefully determined. The diameter of the collimator mounted in front of detector T was measured with a scanning microscope. In the actual measurements, the center of the unscattered beam was first found by maximizing the counting rate in detector T by moving it in both directions. Scattering angles used in thickness measurements were then easily found from the known distance from the beam center as read on the potentiometers.

The actual thickness measurements were carried out by measuring the number of particles scattered into detector T in a sequence of 10-sec intervals, while the current was measured by inserting the Faraday cup between counting periods. Every foil thickness was measured several times. In Table I is shown the results of thickness measurements with different He-ion energies, scattering angles, and singly- and doubly-charged ions. Also different incident ion currents were used. The energies used for computation of the thicknesses were corrected for the small energy loss in the targets. The agreement between the thickness determinations for different energies and scattering angles indicates that, in fact, the Rutherford-scattering law is valid in our case. We conclude that multiple scattering

and atomic screening do not play any role at the scattering angles and energies used to derive the target thicknesses.

The agreement between the thickness measurements in Table I for singly- and doubly-charged He ions is an independent check on the current measurements. The thickness determination is estimated to yield absolute values with an accuracy of 5%.

C. Targets

The targets used were commercially available (Yissum Research Company, Israel) and consisted of thin self-supporting carbon foils (5–25 $\mu\text{g}/\text{cm}^2$) which we mounted on aluminum frames by means of a colloidium film. The nominal thickness values as given by the suppliers were off as much as a factor of 2 from the thicknesses we measured. After the mounting, the colloidium was dissolved with amylacetate. We investigated the targets for impurities by looking at the energy spectrum of 2-MeV He ions Rutherford backscattered from the thin foil. Because of the different elastic energy loss in the scattering event, helium ions scattered from impurity atoms appeared at energies different from those found for ions scattered from carbon atoms. The measurements showed the impurity content of the carbon foil to be quite small, giving rise to an uncertainty considerably smaller than 5% in the half-width of the multiple-scattering distribution.

The thickness of a foil was always measured before as well as after it was used for multiple-scattering measurements. Even after three days' running, no change in thickness could be detected.

III. THEORY

Meyer⁷ has carried out theoretical calculations on multiple scattering for heavy ions in the region where a classical description is applicable. He used the Thomas-Fermi scattering cross section proposed by Lindhard *et al.*,⁸ and defined two dimensionless parameters, namely, a reduced angle $\bar{\vartheta}$ and a reduced thickness τ :

$$\bar{\vartheta} = \frac{\epsilon}{2} \frac{m_1 + m_2}{m_2} \vartheta, \quad (1)$$

$$\tau = \pi a^2 N t; \quad (2)$$

$\epsilon = a/b$ is the dimensionless energy unit introduced by Lindhard *et al.*, where a is a Thomas-Fermi screening parameter which may be given by

$$a = a_0 0.885 (Z_1^{2/3} + Z_2^{2/3})^{-1/2}, \quad (3)$$

and b a collision parameter defined by

$$b = 2 \frac{Z_1 Z_2 e^2}{v^2} \frac{m_1 + m_2}{m_1 m_2}. \quad (4)$$

m_1 and m_2 are the masses of the incident ions (of velocity v) and the target atoms, respectively, N and t are the density and the thickness of the target. (The laborious computations involved in obtaining ϵ and a for each ion-target combination may be avoided by using the tables of Winterbon.⁹)

The main result of the calculations is that the angular distribution measured in reduced angles is independent of the energy of the incident particles, but mainly depends upon the reduced thickness τ .

Meyer derives the following formula for the angular distribution:

$$F(\bar{\vartheta}) = \frac{\epsilon^2}{8\pi} \frac{(m_1 + m_2)^2}{m_2^2} [f_1(\tau, \bar{\vartheta}) - \pi a^2 N^{2/3} f_2(\tau, \bar{\vartheta})]. \quad (5)$$

f_1 and f_2 are given in Ref. 7.

For the τ values used in the present work, the second term containing f_2 in Eq. (5) is negligible and is not considered in the following discussion. The f_2 term is only important for extremely small τ values. As seen from Eq. (5), the half-width (half of the width at half-maximum) of multiple-scattering distributions for different combinations of Z_1 , Z_2 , and incident-ion energy E should fall on a single curve if plotted in the reduced half-width and thickness $\bar{\vartheta}_{1/2}$ and τ (disregarding the second term). This universal curve is shown as a fully drawn line in Fig. 3. From the figure it is seen that for small thicknesses, the half-widths of the distributions are proportional to the thickness, while for larger thicknesses, the half-widths are approximately proportional to the square root of the thickness.

From Eq. (5) it is also possible to obtain the actual shape of the distributions. It is of particular interest to see the deviations from the Gaussian shape. The deviations between the shape of a Gaussian and that of the calculated distributions are small at angles smaller than the half-widths, but significant in the tails of the distributions. The ratio between the intensity of a distribution at an angle equal to the full width at half-maximum and the intensity at the center of the distribution was chosen as a suitably sensitive parameter for the study of the shape of the distributions. In Fig. 4,

TABLE I. The results of thickness measurements using different He-ion energies, scattering angles, and singly- and doubly-charged ions. The indicated errors are due to counting statistics only.

Ion	E (keV)	ϑ	t ($\mu\text{g}/\text{cm}^2$)
He ⁺	300	5.97°	17.3 ± 0.8
He ⁺	350	5.97°	16.3 ± 0.2
He ⁺	400	5.97°	16.1 ± 0.2
He ⁺⁺	400	5.97°	16.5 ± 1.0
He ⁺⁺	400	7.70°	16.0 ± 0.8
He ⁺⁺	500	5.97°	17.3 ± 1.2
He ⁺⁺	500	7.70°	16.0 ± 1.3

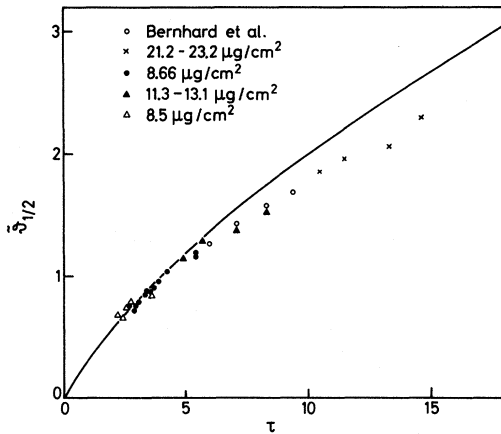


FIG. 3. Experimentally measured half-widths (half the width at half-maximum) as a function of thickness—in reduced units—together with Meyer's (Ref. 7) calculations (solid line). Included are also data of Bernhard *et al.* (Ref. 2). The points are, in order of increasing τ , obtained with the following ions: open circle: all Li^+ ; cross: N^+ , N^+ , Li^+ , Li^+ ; closed circle: Sc^+ , Ar^+ , Cl^+ , S^+ , Al^+ , Mg^+ , Na^+ , Ne^+ , F^+ , N^+ , Li^+ , Li^+ ; closed triangle: Ne^+ , Ne^+ , Li^+ , Li^+ ; open triangle: Zn^+ , Mn^+ , Sc^+ , Ar^+ , Ne^+ .

$I(2\vartheta_{1/2})/I(0)$ is plotted (as calculated from Meyer's tables) as a function of τ . The corresponding ratio of a Gaussian distribution is also shown (dashed line).

The theory assumes negligible energy loss in the target. In our case, the maximum energy losses were about 10% of the incident energies. The energies used to convert to the reduced angle ϑ were the average energies of the ions while penetrating the foils.

For $\tau > 20$, the theoretical predictions of Meyer and Molière agree.⁷ Molière's theory is stated to be valid for thicknesses corresponding to $\tau \geq 20$ only. Keil *et al.*¹⁰ have extended Molière's theory to thicknesses corresponding to $\tau < 20$. A discussion of the various theoretical calculations has been given in Ref. 7.

IV. RESULTS AND DISCUSSION

In his calculations, Meyer assumes that classical mechanics is applicable. Lindhard *et al.*⁸ estimate a classical description of an angular deflection in the applied screened Coulomb potential to be valid when the following inequality is fulfilled:

$$\kappa = \frac{2Z_1 Z_2 e^2}{\hbar v} > 1 + \frac{p^2}{a^2}. \quad (6)$$

Here, p is the impact parameter. We have found that Eq. (6) is fulfilled in all our cases, assuming that the smallest deflections dealt with are equal to the beam divergence. Normally, for large κ values, the inequality [Eq. (6)] is violated only at very small

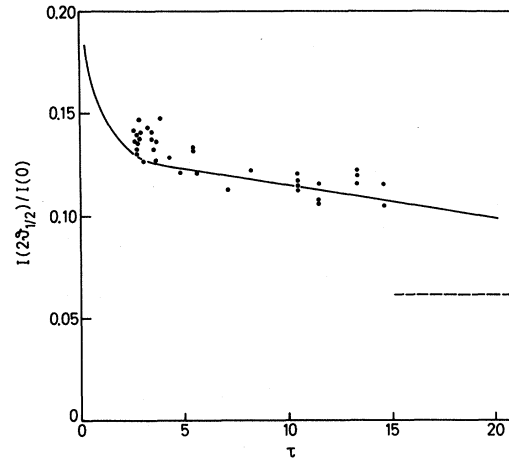


FIG. 4. Experimentally measured values $I(2\vartheta_{1/2})/I(0)$ of the ratio between the intensity at two times the half-width and the intensity at zero scattering angle as a function of τ , together with the theoretical prediction of Meyer (Ref. 7) (solid line). Also the corresponding ratio for a Gaussian distribution is shown (dashed line).

scattering angles.

In Table II, the reduced half-widths (half of the width at half-maximum) obtained from multiple-scattering distributions measured for different ions at different energies are shown. The table shows the reduced half-widths to be independent of energy within the measuring accuracy, implying that the actual half-widths are inversely proportional to energy.

In Fig. 3, the experimentally measured half-widths are plotted in the reduced units $\vartheta_{1/2}$ and τ together with the theoretically predicted half-width. The agreement between theory and experiment is good. At larger τ values, there seems to be a small systematic discrepancy between theory and our experimental data, while for smaller τ values, the experimental data fall almost on the theoretical curve. The small disagreement may be due to the

TABLE II. The experimentally obtained reduced half-widths $\vartheta_{1/2}$ for different ions at different energies. Corrections for energy loss (ΔE) in the foils have been made.

Ion	$E - \Delta E / 2$ (keV)	t ($\mu\text{g}/\text{cm}^2$)	$\vartheta_{1/2}$
${}^7\text{Li}^+$	179	23.3	2.32
...	273	...	2.33
...	371	...	2.31
${}^{14}\text{N}^+$	258	21.2	1.85
...	354	...	1.81
...	547	...	1.85
...	740	...	1.85
${}^{40}\text{Ar}^+$	285	8.5	0.780
...	431	...	0.780
...	676	...	0.795
...	973	...	0.790

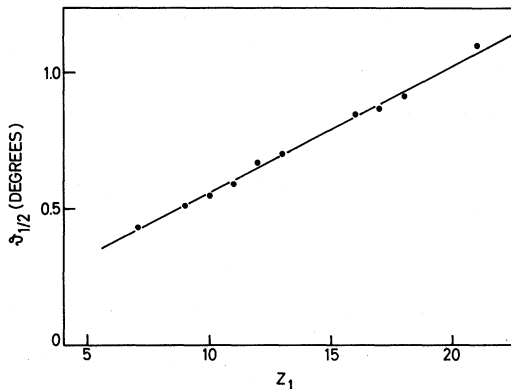


FIG. 5. The measured half-widths (half the width at half-maximum) $\vartheta_{1/2}$ for different heavy ions transmitted through the same foil. In all cases, the incident energy is 500 keV. There have been no corrections for energy loss in the foil. The curve is drawn merely to guide the eye.

choice of potential. This appears reasonable in the light of the findings of Loftager and Claussen.¹¹ They measured the differential cross section and found that the Thomas-Fermi model overestimated the scattering in the entire region where it is significantly different from the Rutherford cross section. However, a weaker potential would cause the half-widths to be smaller, and thus we must conclude that to some extent, the good agreement between theory and experiment for small τ values is fortuitous.

From Fig. 3 it is seen that it is possible to draw a single line through our experimental points, indicating that the reduced parameters $\bar{\vartheta}$ and τ are in fact relevant and very useful. By using the reduced scaling parameters and the experimental curve in Fig. 3, it is possible to obtain the half-width of an angular-scattering distribution for different combinations of target and projectile. This perfect scaling confirms the predictions of Lindhard *et al.*⁸ as to the dependence of a on Z_1 , Z_2 , etc.

In Fig. 4 are shown the measured values $I(2\vartheta_{1/2})/I(0)$ of the ratio of the intensity at twice the half-width and at zero angle as a function of τ , together with the theoretical prediction. The agreement between theory and experiment is good. For larger τ values, it is seen that the distribution becomes increasingly more Gaussian in shape. The agreement between a measured and a calculated distribution is shown in Fig. 2(b).

In Fig. 5 is shown the measured half-width at half-maximum $\vartheta_{1/2}$ for different heavy ions transmitted through the same foil. In all cases, the incident energy is 500 keV. No corrections for energy loss in the foil have been made. All the measured half-widths fall on a single smooth curve. Neither did measurements on other foils show deviations from a smooth, nonoscillating curve. As mentioned

above, there is a close connection between nuclear stopping power and multiple scattering. Recently, it has been proposed¹² that there should be strong oscillations in the nuclear stopping power as a function of Z_1 . The data shown in Fig. 5 indicate that any oscillations are smaller than 5% for the ion-target combinations and energies dealt with here.

In the following, we are limiting the discussion of other experimental data to cases where classical mechanics are applicable, and to thicknesses $\tau < 20$, the region covered by Meyer's calculations, but not treated in detail by Molière. In this region, rather few experimental data are available. Ormrod and Duckworth¹³ have measured the angular distribution for ^{20}Ne transmitted through a $\sim 2\text{-}\mu\text{g}/\text{cm}^2$ carbon foil. Bednyakov *et al.*¹⁴ have measured the angular distribution for keV protons transmitted through thin copper targets. Sakisaka *et al.*¹⁵ have studied the multiple scattering of 1.28- and 2.29-MeV nitrogen ions in evaporated copper targets. In all cases, the agreement between experimental data and Meyer's calculations is reasonably good. More extensive measurements have been carried out by Andersen *et al.*,³ Bernhard *et al.*,² Cline *et al.*,¹⁶ and Högberg *et al.*¹⁷ The data in Refs. 3 and 16 are difficult to compare with Meyer's results because of uncertainty as to the thicknesses used. In both cases, the authors used nominal thickness values as given by the suppliers of the targets. The agreement between the measurements by Bernhard *et al.* and our own results is good, and, in fact, their data help define a common experimental curve (Fig. 3). For larger τ values, the reduced half-widths derived by Högberg *et al.* are somewhat high compared with our measurements. Some of the small discrepancies could be due to the fact that the relative energy losses in the work of Högberg *et al.* are quite high. Furthermore, the larger half-widths are observed for the lighter ions only (H, He); in preliminary measurements with helium ions, we also observe similar high values of reduced half-widths.

V. CONCLUSION

(a) The angular distribution of several heavy keV ions multiple scattered in thin carbon foils has been compared to published experimental results. Where a comparison is possible, the agreement is good.

(b) Experimental data for 13 different ions may be depicted on a single curve by means of reduced angles and thicknesses, constituting an accurate confirmation of the Thomas-Fermi scaling. Furthermore, it shows that the measured half-widths are inversely proportional to projectile energy.

(c) At small foil thicknesses, the numerical agreement with Meyer's theory⁷ is very good, while small systematic deviations are found at larger reduced thicknesses ($\tau > 6$).

ACKNOWLEDGMENTS

We are specially grateful to J. Bjerglund for

operating the heavy-ion accelerator, and to E. Bonderup and G. Sørensen for many fruitful and constructive discussions.

- ¹W. T. Scott, *Rev. Mod. Phys.* **35**, 231 (1963).
²F. Bernhard, J. Lippold, L. Meyer, S. Schwabe, and R. Stolle, *Proceedings of the International Conference on Atomic Collisions Phenomena in Solids* (North-Holland, Amsterdam, 1970), p. 663.
³See, e.g., T. Andersen, K. A. Jessen, and G. Sørensen, *Nucl. Instr. Methods* **90**, 41 (1970).
⁴See, e.g., J. W. Mayer, L. Eriksson, and J. A. Davies, *Ion Implantation of Semiconductors* (Academic, New York, 1970).
⁵N. Bohr, *Kgl. Danske Videnskab. Selskab, Mat.-Fys. Medd.* **18**, No. 8 (1948).
⁶C. Molière, *Z. Naturforsch.* **3a**, 78 (1948).
⁷L. Meyer, *Phys. Status Solidi* **44**, 253 (1971).
⁸J. Lindhard, V. Nielsen, and M. Scharff, *Kgl. Danske Videnskab. Selskab, Mat.-Fys. Medd.* **36**, No. 10 (1968).
⁹K. B. Winterbon, Atomic Energy Commission Laboratory Report No. 3194, 1968 (unpublished).
¹⁰E. Keil, E. Zeitler, and W. Zinn, *Z. Naturforsch.* **15a**, 1031 (1960).
¹¹P. Loftager and G. Claussen, *Proceedings of the Sixth International Conference on the Physics of Electronic and Atomic Collisions* (MIT, Cambridge, Mass., 1969), p. 518; and further unpublished results.
¹²R. S. Nelson, *Phys. Letters* **28A**, 676 (1969).
¹³J. H. Ormrod and H. E. Duckworth, *Can. J. Phys.* **41**, 1424 (1963).
¹⁴A. A. Bednyakov, V. N. Dvoretiskii, I. A. Savenko, and A. F. Tulinov, *Zh. Eksperim. i Teor. Fiz.* **46**, 1901 (1964) [*Sov. Phys. JETP* **19**, 1280 (1964)]; A. A. Bednyakov, A. N. Boyarkina, I. A. Savenko, and A. F. Tulinov, *ibid.* **42**, 740 (1962) [**15**, 515 (1962)].
¹⁵M. Sakisaka, T. Yamazaki, and M. Takasaki, *J. Phys. Soc. Japan* **29**, 1551 (1970).
¹⁶C. K. Cline, T. E. Pierce, K. H. Purser, and M. Blann, *Phys. Rev.* **180**, 450 (1969).
¹⁷G. Högberg, H. Nordén, and H. G. Berry, *Nucl. Instr. Methods* **90**, 283 (1970).

PHYSICAL REVIEW B

VOLUME 4, NUMBER 7

1 OCTOBER 1971

Determination of the Total Momentum Distribution by Positron Annihilation

Chanchal K. Majumdar

Tata Institute of Fundamental Research, Bombay, India

(Received 10 March 1971)

Current experimental techniques of two-photon angular correlation in positron-annihilation studies measure the probability distribution of one or two components of the total momentum of the electron-positron pair. We discuss the problem of deducing the probability distribution of the total momentum itself from the experimental data. It is shown that information about two components of the total momentum can in principle determine the probability distribution of the total momentum.

INTRODUCTION

Several different geometries are used for two-photon angular-correlation experiments in studying positron annihilation in various substances. Let $\rho(\vec{p})$ denote the probability that the total momentum of the two γ rays (and therefore of the annihilating electron-positron pair) is \vec{p} . Now the experiments do not determine $\rho(\vec{p})$ directly, but only the probability distribution of some component of \vec{p} , obtained by suitably integrating over $\rho(\vec{p})$.

The most common setup uses two long slits.¹ This geometry measures the probability that the photon pair has the z component of momentum equal to p_z :

$$N(p_z) = \int_{-\infty}^{\infty} \int_{-\infty}^{\infty} dp_x dp_y \rho(\vec{p}). \quad (1)$$

A second type of setup uses two point counters moving in one plane²; this gives

$$N(p_z) = \int_{-\infty}^{\infty} \int_{-\infty}^{\infty} dp_x dp_y \delta(p_y) \rho(\vec{p}). \quad (2)$$

A variation of this geometry, proposed by Fujiwara,³ uses two pairs of crossed slits, and can give useful information about the Fermi-surface anisotropies.

A new technique recently introduced⁴ uses a point counter together with a spark chamber. The line joining the sample to the point counter defines the z axis; the plates of the spark chamber are parallel to the xy plane. This geometry yields

$$N(p_x p_y) = \int_{-\infty}^{\infty} \rho(\vec{p}) dp_z. \quad (3)$$

In each case, one can try to determine $\rho(\vec{p})$ itself from the experimental data. In this paper we shall discuss the mathematical solution of this problem. In particular, we describe how the data supplied by Eq. (3) can be analyzed to yield $\rho(\vec{p})$.

This problem for the two long slits was discussed